Cohesive properties and electronic structure of Heusler $L2_1$-phase compounds Ni_2XAl (X = Ti, V, Zr, Nb, Hf, and Ta)

W. Lin and A. J. Freeman
Department of Physics and Astronomy, Northwestern University, Evanston, Illinois 60208-3112
(Received 27 June 1991)

The ternary (Heusler) $L2_1$-phase compounds Ni_2XAl (group-IVA or -VA element X=Ti, V, Zr, Nb, Hf, and Ta) have been found to greatly increase the high-temperature creep strength of NiAl. We report here the cohesive properties and electronic structures of these potential high-temperature structural materials in both the Heusler $L2_1$ and the $B2$ phases determined by means of the all-electron total-energy self-consistent linear muffin-tin orbital method based on the local-density approximation. Our results show that the calculated equilibrium lattice constants of the $L2_1$-structure compounds are in very good agreement with experiment. For Ni_2TiAl and Ni_2VAl, the lattice constants are found to match that of NiAl (mismatch is 1.7% and 1.0%, respectively). But for the other four compounds, the mismatch is found to be larger (3.6–5.6%). The difference of the lattice constants in the $B2$ and the $L2_1$ structures, however, is very small (less than 1%). The formation energy is found to be consistently in favor of the $L2_1$ phase. The Ni d and X d hybridization contributes the most to the cohesion of these compounds whose stability is also made certain by the well-separated filled bonding and empty antibonding states in the density of states. The density of states of the $B2$ phase is quite similar to that of $L2_1$, but distinctions exist due to their structural differences. The rigid-band approximation is found to work well for these compounds.

I. INTRODUCTION

The $L2_1$-structure compounds (also known as the Heusler compounds), with nominal composition formula A_2BC, have long been known as an important stable structure for certain ternary compounds. $L2_1$ has a unique close-packed cubic structure unit cell composed of eight simple bcc (B_2) unit cells (cf. Fig. 1). While the Heusler phase compounds were well known for their ferromagnetic properties (even when the constituent elements are not ferromagnetic),[1] paramagnetic $L2_1$ compounds also exist widely. In this category, NiAl is known to form stable $L2_1$ compounds with the group-IVA and -VA elements (Ti, V, Zr, Nb, Hf, and Ta); among them, Ni_2TiAl is the most studied. Early experiments[2] on Ni_2TiAl showed its role in forming multiphase compounds with Ni-rich binary compounds (e.g., Ni_3Ti and Ni_3Al).

Recently, the intermetallic compound NiAl has been discovered to possess desirable features (high melting temperature, good oxidation resistance, low density) as a potential structural material in the aerospace industry. Thus extensive efforts have been focused on solving its weaknesses, namely, the low ductility at room temperature and loss of strength at higher temperatures (>600 °C). Including ternary elements in NiAl was found to be one of the most effective ways of solving these problems. In particular, the $L2_1$ phase Ni_2XAl (X=Ti, V, Zr, Nb, Hf, and Ta) compounds have attracted much attention since Ti was reported to strengthen NiAl at high temperature by forming $L2_1$ structured Ni_2TiAl.[3–6] The dual phase NiAl/Ni_2TiAl can increase the creep strength of NiAl by a factor of 3 (Ref. 7) which results in

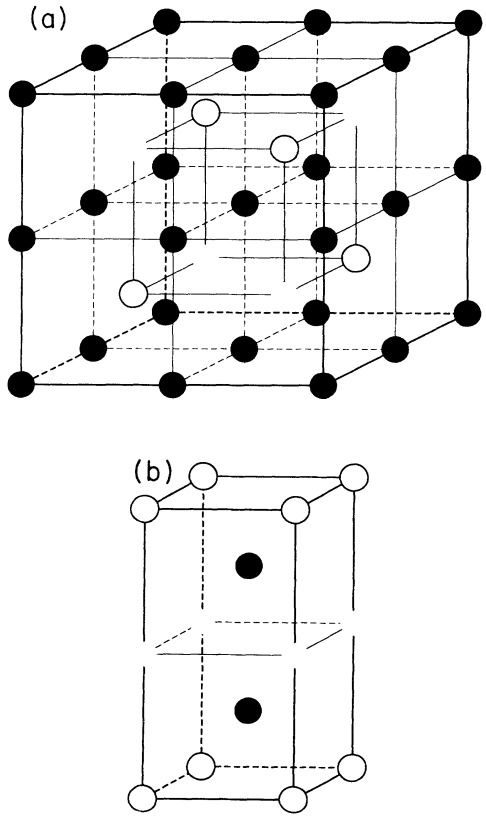

FIG. 1. The unit cell of the (a) $L2_1$ Heusler and (b) $B2$-like phase structure. The filled, shaded, and empty circles represent Ni, X, and Al atoms, respectively (X stands for Ti, V, Zr, Nb, Hf, and Ta).

a strength comparable to the Ni-based γ/γ' superalloy.[8,9] This is a strength far superior to single phase intermetallic compounds alone. Furthermore, $B2$ NiAl and $L2_1$ Ni_2TiAl are found to have small lattice mismatch and the stability of Ni_2TiAl is reported to be very good.[6] A connection between its high strength and stability has been made.[10] Although the $L2_1$ phase Ni_2TiAl is found to have only limited ductility[11] at room temperature, boron has been shown to be able to increase the grain boundary cohesion,[12] as it does in Ni_3Al. Further studies on multiphase compounds such as the combination of $L2_1$-$B2$-$L1_2$ (β'-β-γ) phase compound of Ni_2TiAl-Ni(Al,Ti)-Ni_3(Al,Ti) show signs for both good creep strength at high temperature and improved ductility at room temperature.[13] Interestingly, Ni_2VAl is found to have almost zero lattice mismatch between its $B2$ and $L2_1$ phases.[14] The elements Hf, Ta, and Nb are also found to have second phase strengthening[15] in NiAl. Both Ni_2HfAl (Ref. 11) and Ni_2TaAl (Ref. 16) were experimentally tested to be very hard. In Ni_2HfAl (and possibly in other similar compounds), the high shear modulus due to the internal "lattice strain"[11] is thought to be responsible for its hardness (8.3 GPa) which in turn produces less diffusion and greater creep strength.

On the other hand, very little has been known theoretically for these $L2_1$ phase compounds besides recent studies on the phase diagrams of NiAl/Ni_2TiAl by the CVM method.[17,18] Many questions concerning the cohesive and electronic properties, for example, the phase stability of these $L2_1$ Heusler compounds and the lattice mismatch between NiAl and Ni_2XAl compounds, remain unanswered. Meanwhile, it is also interesting to study how ternary additions affect the structural and electronic properties of binary NiAl. To our knowledge, no first-principles theoretical study has been reported for these purposes in Ni_2XAl. In this paper we studied six Heusler phase Ni_2XAl compounds (X = Ti, V, Zr, Nb, Hf, and Ta) and four $B2$-like compounds with the same nominal composition formula Ni_2XAl (X=Ti, V, Zr and Nb) for their cohesive properties and electronic structure. Comparisons between the $B2$ structure compounds and their $L2_1$ counterparts are made. Cohesive properties of NiAl and NiTi from related studies are given and compared with Ni_2TiAl. The total and partial density of states are also presented and examined.

II. THEORETICAL APPROACH

Based upon the local-density approximation (LDA)[19] within density functional theory, the electronic structures were studied by the all-electron self-consistent linearized muffin-tin orbital (LMTO) method[20] within the atomic sphere approximation (ASA). The combined correction terms were added in all calculations to improve accuracy. The Hedin-Lundqvist form of the exchange-correlation potential[21] was used and spherical harmonic functions were included up to $l=2$ (d orbital). The f electrons in Hf and Ta were treated as core electrons which were calculated fully relativistically; the spin-orbit coupling was neglected for the valence electrons. For simplicity we assumed that all atoms have the same Wigner-Seitz (WS) radius. The total energies are defined at 0 K, i.e., no entropy contribution is included. Sampling **k** points were constructed in the irreducible Brillouin zone (IBZ) by means of the linear tetrahedron method; 30 **k** points were generally used in our calculation for the $L2_1$ and $B2$ phases. The formation energy was calculated by subtracting the sum of the total energies for the constituent metals from the total energy of the compounds, $\Delta E = E_{M_aN_b} - (aE_M + bE_N)$.[22] The equilibrium lattice constants for the $L2_1$ and $B2$ structures were determined by the total energy minimum versus total volume.

The unit cells of the Heusler $L2_1$ and $B2$-like structures for Ni_2XAl are shown in Figs. 1(a) and 1(b); the filled, shaded, and empty circles are Ni, X, and Al atoms, respectively. In Fig. 1(a), the $L2_1$ structure has 16 atoms in the unit cell. This is a close-packed complex cubic structure in which the Ni atoms occupy corners as well as body, face, and edge centers, and the Al and X atoms occupy the eight (1/4,1/4,1/4) positions. $L2_1$ can also be treated as a combination of eight simple $B2$ unit cells (four NiAl and four NiX cells with Ni occupying the corner positions, and Al or X occupying the body-centered position of the simple $B2$ cell, respectively) with two different types of the basic $B2$ cells (NiAl or NiX) at adjacent positions. Due to the way NiAl and NiX cells pile up, the nearest-neighbor (basic $B2$) cells are always the other type.

The $B2$-like unit cell [shown in Fig. 1(b)], on the other hand, is a stack-up of only two different types of basic $B2$ unit cells with $c/a=2$, although in real compounds the distribution of X atoms can be in a random fashion, i.e., disordered. We assume in our calculation that the $B2$-like compound retains its long-range order. Thus, similar to the ternary $L1_2$ structure,[23] the ternary $B2$ cell can be described as the piling up of two bcc NiAl cells with X substituting the Al positions in the middle plane. Note that this unit cell is also one quarter of the $L2_1$ unit cell [cf. Fig. 1(a)]. Four of these cells can compose an $L2_1$ structure by combining them side by side (shift two of the cells by half of their height). Thus the ternary $B2$ Ni_2XAl phase can actually be viewed as an intermediate phase between $B2$ NiAl and $L2_1$ Ni_2XAl. Also in $B2$ Ni_2XAl, in contrast to the $L2_1$ phase, the adjacent basic $B2$ cells (i.e., NiAl or NiX) have four in the same type and only two in the different type of cells.

III. RESULTS AND DISCUSSION

A. Equilibrium lattice constants and formation energies

The calculated and experimental equilibrium lattice constants, their mismatch to that of NiAl and the formation energy of these Heusler phase compounds are listed in Table I. For the equilibrium lattice constants we found that the calculated results are in very good agreement with all available experimental data except for Ni_2VAl. The error is generally within 1% which is considered within the error due to the LDA. Ni_2TiAl is of special interest because it has the same nominal composi-

TABLE I. The calculated and observed equilibrium lattice constants (a) of the Heusler $L2_1$ phase Ni_2XAl (X=Ti, V, Zr, Nb, Hf, and Ta) compounds, the lattice mismatch between $L2_1$ Ni_2XAl and NiAl, and their formation energies ($E_{formation}$). The related data of NiAl and NiTi are also listed.

Compound	a (calc.) (Å)	a (expt.) (Å)	Mismatch (%)	$E_{formation}$ (mRy/atom)
Ni_2TiAl	5.87	5.872,[a] 5.843[d]	1.7	63.0
Ni_2VAl	5.78	6.33[d]	1.0	47.5
Ni_2ZrAl	6.10	6.123[a,d]	5.6	61.2
Ni_2NbAl	6.00	5.974,[a] 5.970[d]	3.9	50.9
Ni_2HfAl	6.10	6.081,[a,d] 6.07[b]	5.6	69.7
Ni_2TaAl	5.95	5.945,[a] 5.936,[c] 5.949[d]	3.0	57.8
NiAl	2.88	2.887[d]	0.0	71.0
NiTi	3.00	3.015[d]	3.9	35.0
NiTi+NiAl				53.0

[a]Reference 1.
[b]Reference 11.
[c]Reference 16.
[d]Reference 24.

tion formula as the combination of NiAl and NiTi. The corresponding calculated equilibrium properties are also listed in Table I. We found that the equilibrium lattice constant for Ni_2TiAl is 5.87 Å. In addition to its agreeing within 0.5% error with the observed value, it is also right in between twice that of NiTi [6.00 Å (calculated)] and NiAl [5.76 Å (calculated)]. Thus in a general sense, Vegard's law[25] is preserved. In the case of Ni_2VAl, the theoretical equilibrium lattice constant is found to be 5.78±0.01 Å which is quite different from the only set of experimental results available [6.33 Å (cf. Table I)]. However, as will be discussed later, Ni_2VAl may exist in an $L2_1$ and $B2$ mixed phase due to their small formation energy difference, which would cause difficulty in obtaining accurate experimental results[14] for the lattice constant of pure $L2_1$ Ni_2VAl. Finally, the lattice constants for the other four compounds Ni_2XAl (X=Zr, Nb, Hf, and Ta) are in excellent agreement with experiment. Note that since the heavier elements Zr, Nb, Hf, and Ta have larger atomic radii than Ti and V have, it is not surprising to see that they form compounds with larger lattice constants.

The lattice mismatch is defined as the percentage of the difference between the lattice constant of the Heusler phase and that of two times $B2$ NiAl. We used our calculated lattice constants to compute the mismatch and the lattice constant of NiAl (2.88 Å) was used as reference. As expected, we found that the mismatch for the Ti and V Heusler phase compounds is small (1.7 and 1.0%, respectively). The mismatch for the other four compounds is much larger (cf. Table I) which corresponds very well to available experimental results. The mismatch is generally larger for group-IVA elements (5.6% for both Zr and Hf Heusler compounds) than that of group-VA elements (3.9% for Nb and 3.0% for Ta Heusler compounds). This fact can also be understood from the group-IVA elements having larger atomic radii. The difference between these atomic radii is speculated to create a "strained lattice,"[11] in other words, one sublattice (e.g. NiTi) is squeezed and the other sublattice (e.g., NiAl) is expanded. Such an internal strain is thought to make these compounds very hard and brittle. However, the large shear modulus would, in turn, decrease the diffusion rate and increase the creep strength.[10] As our results indicate, there is a larger lattice strain and mismatch caused by heavier ternary elements (Zr, Nb, Hf, and Ta) in Ni_2XAl than that caused by Ti and V.

The formation energies of these compounds are found to be fairly large [in between that of NiAl and NiTi (cf. Table I)]. The compounds with group-IVA elements are found to have larger formation energies than those with group-VA elements. A comparison between binary NiAl, NiTi, and Ni_2TiAl shows that while the average formation energy per atom for NiAl and NiTi combined is 53.0 mRy/atom (cf. Table I), the formation energy for Ni_2TiAl is 63.0 mRy/atom. Thus, the formation of Ni_2TiAl from NiAl and NiTi is energetically favored since 10.0 mRy/atom will be released. This is in good agreement with experiment (7.4 mRy/atom[18]) and other calculations (9.0–9.6 mRy/atom[18]). Meanwhile, for the same reason, the creation of the Heusler phase should also be possible in NiAl by adding Ti to Al sites. Among the other Heusler compounds, except for Ni_2VAl which has the smallest formation energy (47.5 mRy/atom), their good phase stability is also assured by their large formation energies which are comparable to that of Ni_2TiAl (cf. Table I).

For the $B2$-like ternary Ni_2XAl compounds, the cohesive properties were also calculated for X=Ti, V, Zr, and Nb. The results are listed in Table II. As stated before, we assume the compounds to have an ordered arrangement for their atoms [cf. Fig. 1(b)]. Surprisingly, the equilibrium lattice constants of these compounds are found to be very close to that of the Heusler phase. In nearly every one of the cases considered, the lattice mismatch between the $B2$ and $L2_1$ phases (cf. Table II) is equal to or less than 1.0%. Especially for Ni_2VAl, this mismatch is indeed found to be ~0.0% (subject to the er-

TABLE II. The calculated equilibrium lattice constants (a) of the $B2$ phase Ni_2XAl (X=Ti, V, Zr, and Nb) compounds (note that in $B2$-like structure, $b=a$ and $c=2a$), the lattice mismatch between the $L2_1$ and $B2$ phases, the formation energies ($E_{formation}$) of the $B2$ phase and the difference between the formation energy of the $B2$ and $L2_1$ phases (ΔE).

Compound	a (calc.) (Å)	Mismatch (%)	$E_{formation}$ (mRy/atom)	ΔE (mRy/atom)
Ni_2TiAl	2.95	0.5	54.7	8.3
Ni_2VAl	2.89	0.0	42.5	5.0
Ni_2ZrAl	3.08	1.0	43.7	17.5
Ni_2NbAl	3.02	0.7	38.5	12.4

ror inherent in the computational method) as found in previous experiments.[14] The formation energy of the $B2$ compounds, on the other hand, is found to be much smaller than that of the Heusler phase compounds. Again taking Ni_2TiAl as an example, its formation energy in the $B2$ phase (54.7 mRy/atom) is 8.3 mRy/atom smaller than that of the $L2_1$ Heusler phase (63.0 mRy/atom), and only 1.7 mRy/atom larger than that of the combined NiAl+NiTi (53.0 mRy/atom). Thus it is feasible for $B2$ Ni_2TiAl to act as an intermediate phase in the $B2$-$L2_1$ transformation, i.e., NiAl and NiTi adjust their lattice constants to form the $B2$ phase first (without changing by much the total energy), then release energy and form the $L2_1$ phase without varying the lattice constant. In the case of Ni_2VAl, the energy difference between the $B2$ and $L2_1$ phases is the smallest (5.0 mRy/atom) among these compounds and suggests the possibility of forming a mixed $B2$ and $L2_1$ phase compound instead of a pure $L2_1$ compound. For the other two $B2$ compounds, Ni_2ZrAl and Ni_2NbAl, the energy differences are considerably larger (17.5 and 12.4 mRy/atom, respectively); thus they should be more stable in their $L2_1$ Heusler phase.

B. Density of states

The density of states (DOS) of the six Heusler compounds Ni_2XAl (X=Ti, V, Zr, Nb, Hf, and Ta) are plotted in Fig. 2. The total and three site projected DOS are shown in the same plot. The remarkable feature is that the total DOS of each of the six compounds is very similar despite the fact that they are composed of different elements from different rows in the periodic table. Thus, the rigid-band model appears to work well in these compounds.

The hybridization is found to be very strong; as a matter of fact, it creates three distinct valleys in the DOS of all six compounds [labeled as A, B, and C in Fig. 2(a)]. Valley B is relatively shallow, but valleys A and C are so deep that they created or almost created semiconductor-like gaps in the DOS [see valley A for Ni_2VAl in Fig. 2(b), valley C for Ni_2TiAl, Ni_2ZrAl, and Ni_2NbAl in Figs. 2(a), 2(c), and 2(d), respectively]. This feature indicates that the interaction between the constituent atoms is strong and that aspects of covalent bonding should exist. Overall, the bonding and antibonding regions can be roughly but clearly separated in these compounds by valleys A and B. The main bonding region is below valley A and the antibonding region is above valley B. Electron states from Ni and X elements are found to have the largest contributions to the DOS. The main peak below E_F in the bonding region consists of continuous high and narrow peaks made up mostly of Ni components. Above E_F, the antibonding peaks are dominated by the X component and are relatively smaller (except for Ni_2VAl, whose antibonding peak is as high as the bonding peak). The compounds with heavier elements (Zr, Nb, Hf, and Ta [cf. Figs. 2(c)–2(f)]) have broader peaks than those with lighter elements [Ti and V (cf. Figs. 2(a) and 2(b)]. Furthermore, in between valleys A and B, there exists a distinguishable nonbonding region with a double-peak structure in the DOS due to the transition from Ni to X states. In all six Heusler compounds, the Fermi level is located in this region. Although Al does not make a dominant contribution in these compounds, it is found to participate in the hybridization throughout the entire energy region (especially in the bonding part).

The bonding region in these compounds [cf. Fig. 2(a)] is completely filled with electrons and the antibonding region is left completely empty. Thus the stability of these compounds is thought to be very good according to Freidel's bonding model.[26] A more detailed analysis shows that in the nonbonding region, while the group-IVA elements only allow E_F in their Heusler compounds to be located near the local minimum between two peaks [cf. Figs. 2(a), 2(c), and 2(e)], the Heusler compounds with group-VA elements have a slightly higher E_F which almost enters the antibonding region [cf. Figs. 2(b), 2(d), and 2(f)]. Thus, compared with the Heusler compounds with IVA elements, the formation energy of the Heusler compounds with VA elements may be reduced by the occupation of some antibonding states. It is also obvious from this point of view that the elements which have more valence electrons than the group-VA elements are less likely to form in the stable Ni_2XAl Heusler phase since its Fermi level will lie in the antibonding region. On the other hand, elements with fewer valence electrons than the group-IVA elements can still be stabilized by locating E_F in the deep valley A in the DOS.

The number of electrons per atom (n_e) values corresponding to the two distinct valleys A and B near E_F in the DOS are listed in Table III. It is found that although

TABLE III. Values of the number of electrons per atom (n_e) corresponding to the two distinct valleys A and B [cf. Figs. 2(a) and 4(a)] in the DOS of the $L2_1$ and $B2$ structured Ni_2XAl (X=Ti, V, Zr, Nb, Hf, and Ta) compounds.

	$L2_1$		$B2$	
Compound	Valley A	Valley B	Valley A	Valley B
Ni_2TiAl	6.00	7.07	6.00	7.99
Ni_2VAl	6.00	7.08	6.00	7.99
Ni_2ZrAl	6.00	7.06	6.00	7.98
Ni_2NbAl	6.00	7.06	6.00	8.00
Ni_2HfAl	6.00	7.07		
Ni_2TaAl	6.00	7.07		

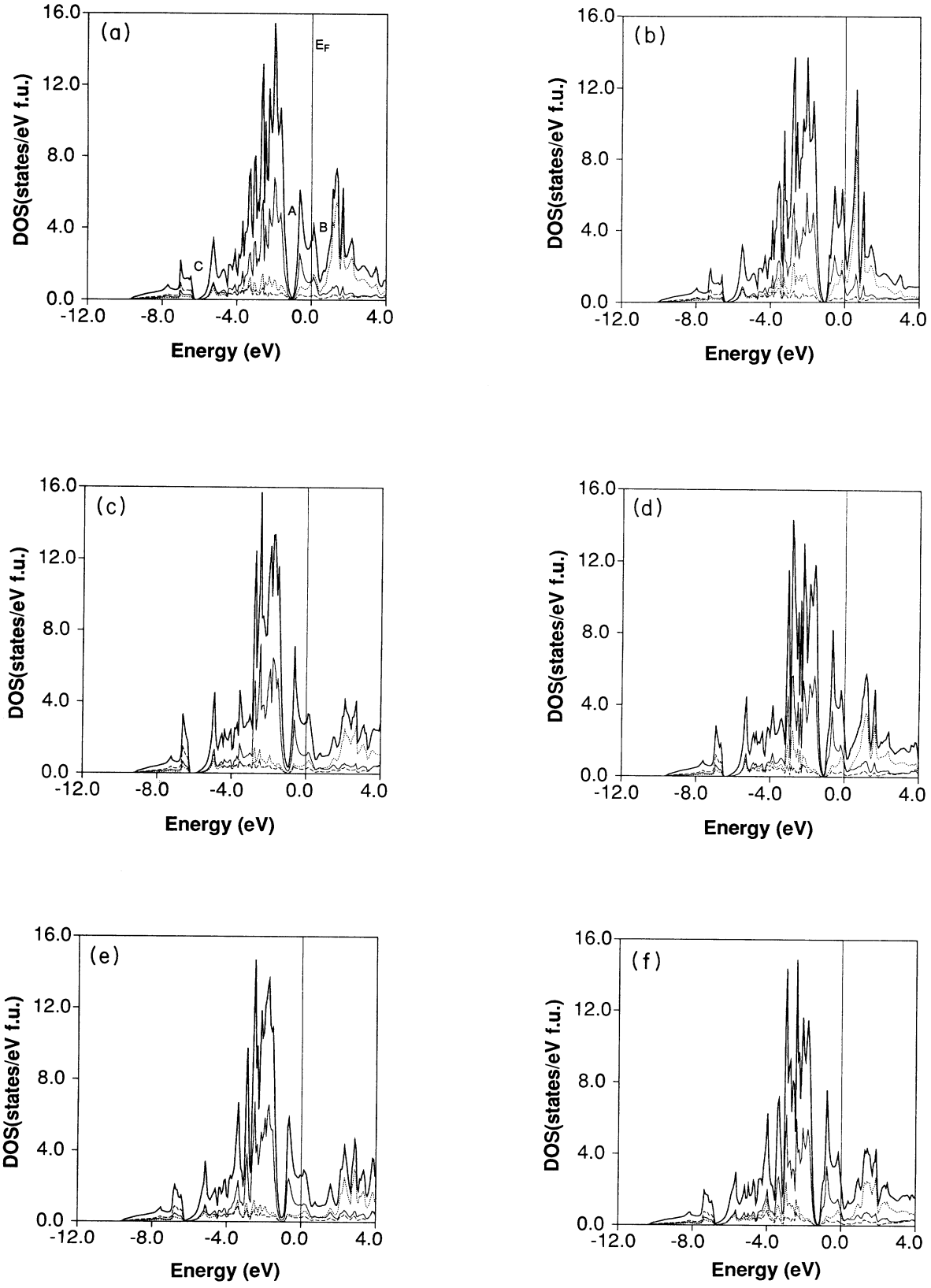

FIG. 2. Total and projected site DOS of the $L2_1$ Heusler phase Ni_2XAl (X=Ti, V, Zr, Nb, Hf, and Ta). The thick solid line denotes the total DOS, and the thin solid, dotted, and broken lines represent the site DOS (in states/eV atom) of Ni, X, and Al, respectively. (a) Ni_2TiAl, (b) Ni_2VAl, (c) Ni_2ZrAl, (d) Ni_2NbAl, (e) Ni_2HfAl, and (f) Ni_2TaAl.

the band becomes narrower for the heavier elements, the number of electrons that fill up the electron states to the valleys are almost unchanged. For "gap" A [cf. Fig. 2(a)], the n_e values are almost always 6.0, and for "gap" B, they are near 7.07. A Heusler phase compound with its n_e value in between these two numbers should be found as one of the most stable. In our case, the n_e values of 6.75 for Ni_2XAl (X=Ti, Zr, and Hf) and 7.0 for Ni_2XAl (X=V, Nb, and Ta) belong to the desired values. The nearly constant n_e values in these compounds again proves the validity of the rigid-band approximation.

As a sample result for the Heusler compounds, the partial DOS of Ni_2TiAl is shown in Fig. 3; here the Ni, Ti, and Al site DOS are decomposed by angular momentum. It is clearly seen that the contribution from the p component of both Ni and Ti is small and spread out on both sides of E_F [cf. Figs. 3(a) and 3(b)]. On the other hand, the Ni- d electrons [cf. Fig. 3(a)] make the dominant contribution to the DOS throughout the whole energy spectrum. The Ni s electrons participate only at low energy (about -5.0 to -8.0 eV). For Ti [cf. Fig. 3(b)], the d component not only dominates the antibonding region, but also contributes the most in the bonding region. However, peculiarly, the Ti s states have a recognizable peak at about -3.0 eV. For Al [cf. Fig. 3(c)], the p electrons dominate the entire region except for the low-energy region (-6.0 to -8.0 eV) where the s electrons appear to have a recognizable peak resulting in the deep valley C [cf. Fig. 2(a)]. Nevertheless, the Ni d and Ti d hybridization makes the major contribution to the cohesion of the compounds.

For $B2$-like Ni_2XAl (X=Ti, V, Zr, and Nb), the total and projected site DOS are shown in Fig. 4 and the DOS decomposed by the angular momentum is shown in Fig. 5. The general features of the DOS are very similar to those of the Heusler phase. The deep valleys A and B still exist; but distinctly different from the $L2_1$ phase—the valley C is not found. The bonding region is still dominated by Ni d and the antibonding region by X d. The Fermi level is also located in the nonbonding region. Although the position of E_F is found to lie relatively lower in energy than in the $L2_1$ structure [e.g., compare Figs. 2(a) and 4(a)], the electrons in these compounds still completely occupy the bonding states and leave the antibonding states empty. Compared to the $L2_1$ compounds, the band width of the $B2$ compounds is found to be generally greater in the nonbonding region (almost twice that of the Heusler phase). This character is better shown by the number of electrons in the nonbonding region (cf. Table III). In the $B2$-like structure, as in the $L2_1$ structure, the n_e corresponding to the valley A [cf. Fig. 4(a)] is still about 6.0. But for valley B, the n_e is about 8.0 instead of 7.07 in the $L2_1$ structure. Thus in the $B2$-like structure, about one extra electron per atom is accommodated in the nonbonding region.

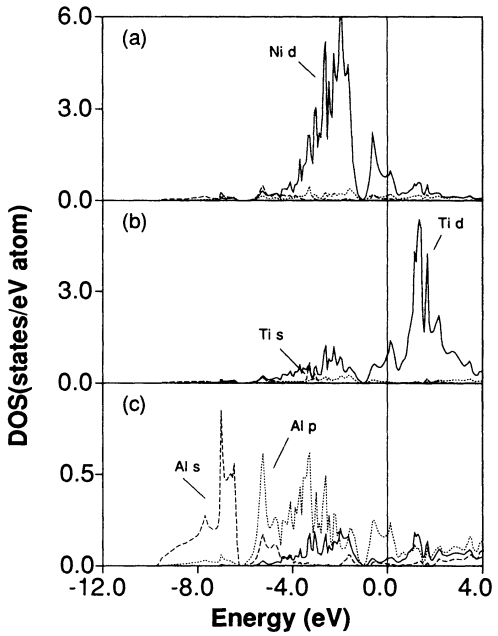

FIG. 3. The partial DOS of Ni, Ti, and Al in $L2_1$ Ni_2TiAl: (a) Ni site, (b) Ti site, and (c) Al site. The solid, dotted, and broken lines represent d-, p-, and s-electron states, respectively.

C. Discussion

These differences in the electronic structure can be related to the structural difference between these two phases (cf. Table IV). Note that the type and number of the first nearest neighbors in these two compounds are the same for all three types of atoms (with possibly different configurations). However, the second nearest neighbors are quite different: for Ni, the second nearest neighbors are the same in both compounds (6 Ni atoms); for X (or Al), there are four same-type atoms and only two different-type atoms in the second neighbor positions in the $B2$ phase; however, the six second neighbors are all different in the Heusler phase (the third nearest neighbors are also listed in Table IV but are not considered important here since they are much farther away than are the second nearest neighbors). Therefore, compared to the $B2$-like compounds, there is an enhanced X-Al second nearest-neighbor interaction in the Heusler compounds due to the structural differences. This interaction considerably affects the electronic structure, i.e., the creation of valley C and a narrower nonbonding region in the $L2_1$ structure [cf. Fig. 2(a)] as well as the cohesive properties. As found previously,[27] our results suggest that the cohesion enhancement in the $L2_1$ phase is correlated to the increase of the X-Al (e.g., Ti-Al) hybridization (especially between s electrons) and possibly to the different arrangement of the first nearest-neighbor X and Al configurations around Ni.

IV. SUMMARY

For all six Heusler $L2_1$ structure compounds, Ni_2XAl (X=Ti, V, Zr, Nb, Hf, and Ta), the calculated lattice constants are found to be in very good agreement with experiment (the error is less than 1% except for Ni_2VAl). The lattice mismatch calculated between NiAl and these $L2_1$ compounds is very small (1.7 and 1.0%, respectively) for

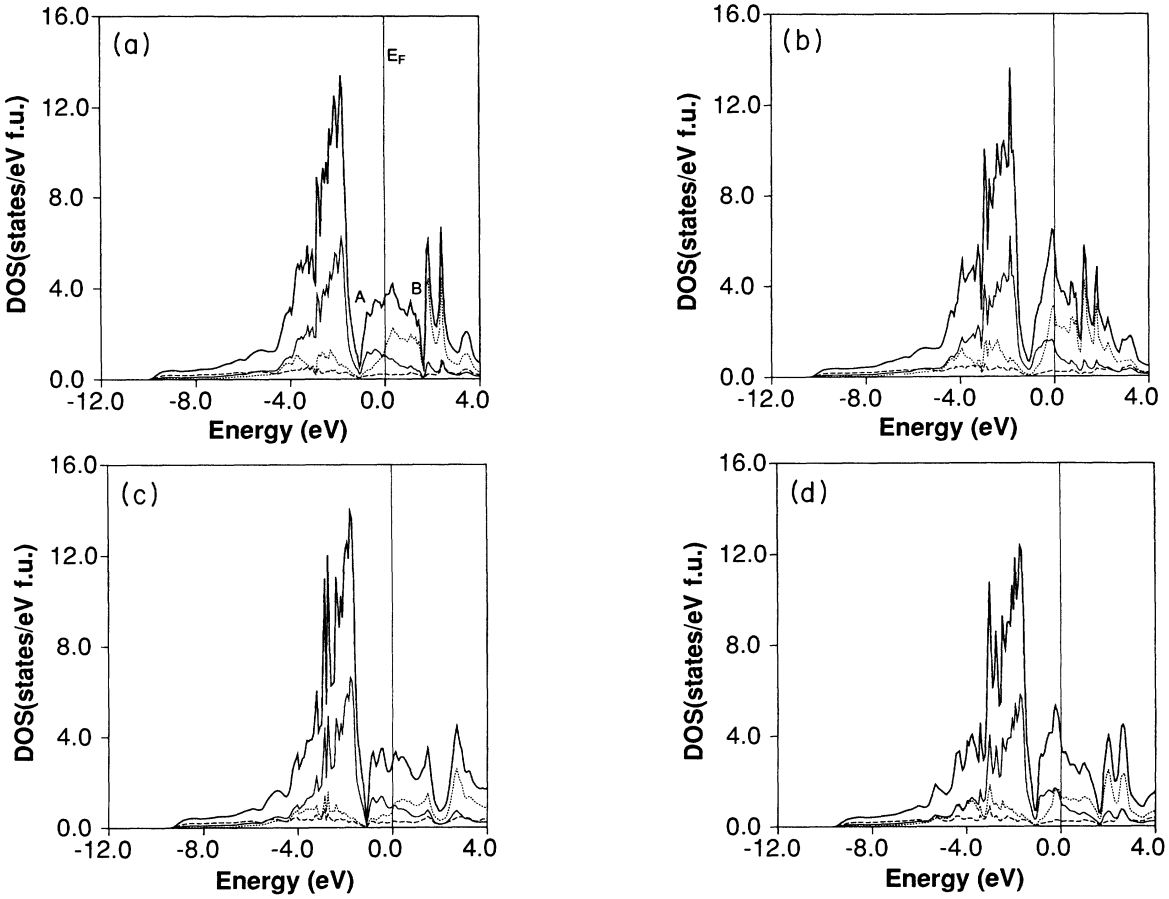

FIG. 4. Total and projected site DOS of the $B2$ phase Ni_2XAl (X=Ti, V, Zr, and Nb). The thick solid line denotes the total DOS, and the thin solid, dotted, and broken lines represent the site DOS (in states/eV atom) of Ni, X, and Al, respectively. (a) Ni_2TiAl, (b) Ni_2VAl, (c) Ni_2ZrAl, and (d) Ni_2NbAl.

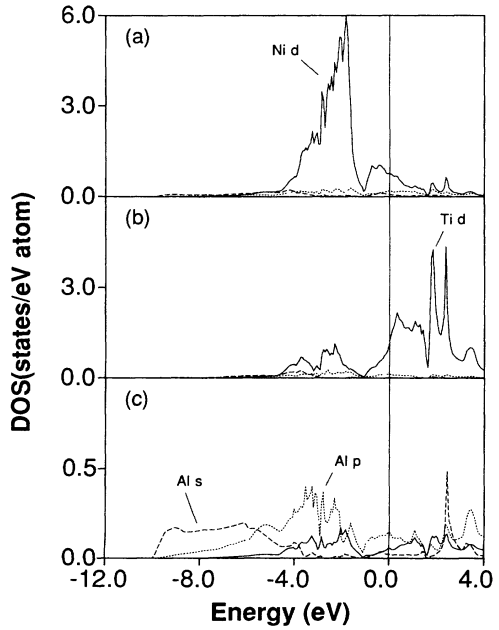

FIG. 5. The partial DOS of Ni, Ti, and Al in $B2$-like Ni_2TiAl. (a) Ni site, (b) Ti site, and (c) Al site. The solid, dotted, and broken lines represent d-, p-, and s-electron states, respectively.

Ni_2TiAl and Ni_2VAl. Therefore, they have the potential to coexist coherently with NiAl. For the other four compounds, in agreement with experiment, the mismatch is fairly large (5.6%, 3.9%, 5.6%, and 3.0% for Zr, Nb, Hf, and Ta, respectively) which causes large lattice strains. The cohesive energy is found to be large for these com-

TABLE IV. Comparison of number of the first, second, and third nearest neighbors (NN) of Ni, X, and Al atoms in the $L2_1$ and $B2$ structured Ni_2XAl compounds (X=Ti, V, Zr, Nb, Hf, and Ta).

Structure	Atom	First NN	Second NN	Third NN
$L2_1$	Ni	4X	6Ni	12Ni
		4Al		
	X	8Ni	6Al	12X
	Al	8Ni	6X	12Al
$B2$	Ni	4X	6Ni	12Ni
		4Al		
	X	8Ni	4X	4X
			2Al	8Al
	Al	8Ni	4Al	4Al
			2X	8X

pounds. In the case of Ni_2TiAl, the calculated formation energy is -10.0 mRy/atom smaller than the combination of NiTi and NiAl. From the density of states of the $L2_1$ phase, it was found that the hybridization is strong. The interaction between constituent atoms creates deep valleys which separate the bonding and antibonding regions. The Fermi level, always located in the nonbonding region, divides the DOS into the completely filled bonding region and empty antibonding region which further assures the stability of these Heusler compounds. The lattice strain and good phase stability in these compounds undoubtedly contribute to the high creep strength. Nevertheless, the semiconductorlike valleys (or "gaps") imply strong covalentlike bonding and may result in poor ductility. The rigid-band approximation also works well for these compounds; the n_e values at two distinct valleys A and B [cf. Fig. 2(a)] in the DOS are almost constant (6.0 and 7.07) for the $L2_1$ phase compounds.

The four ternary compounds in the $B2$-like phase with the same nominal composition formula Ni_2XAl (X=Ti, V, Zr, and Nb) have also been studied for comparison. The lattice mismatch between the $B2$ and $L2_1$ phases is found to be very small (typically less than 1%). The total energy of the $B2$ phase is found to be consistently higher than that of the $L2_1$ phase (difference: 5.0–17.5 mRy/atom). But in the case of Ni_2VAl, the smallest energy difference between the $B2$ and $L2_1$ phases (5.0 mRy/atom) infers a less stable situation for its Heusler phase. The DOS of the $B2$-like phase is akin to that of the $L2_1$ phase. But some unique features are distinctly different: (a) its nonbonding region is found to be much wider than that of the $L2_1$ phase and can hold about one more electron per atom and (b) the distinct valley in the low energy side (~ -6.0 eV) of the DOS in the $L2_1$ phase (mostly due to the s electrons) is not found in the $B2$ phase. These differences are thought to be due to the different second nearest-neighbor X-Al interactions between these two structures.

ACKNOWLEDGMENTS

This work was supported by the Air Force Office of Scientific Research (Grant No. 88-0346) and by a computing Grant at the Wright-Patterson Air Force Base Supercomputer Center. We are grateful to D. M. Dimiduk for helpful discussions.

[1] *Intermetallic Compounds,* edited by J. H. Westbrook (Wiley, New York, 1967).
[2] A. Taylor and R. W. Floyd, J. Inst. Met. **81**, 25 (1952).
[3] R. S. Polvani, W. S. Tzeng, and P. R. Strutt, Metall. Trans. **A7**, 33 (1976).
[4] J. D. Whittenberger, R. K. Viswanadham, S. K. Mannan, and K. S. Kumar, in *High-Temperature Intermetallic Ordered Alloys III,* MRS Symp. Proc. Vol. 133, edited by C. T. Liu, A. I. Taub, N. S. Stoloff, and C. C. Koch (MRS, Pittsburgh, 1989), p. 621.
[5] M. Yamaguchi, Y. Umakoshi, and T. Yamane, Philos. Mag. **A50**, 205 (1984).
[6] Y. Umakoshi, M. Yamaguchi, and T. Yamane, Philos. Mag. **A52**, 357 (1985).
[7] P. R. Strutt, R. S. Polvani, and J. C. Ingram, Metall. Trans. **A7**, 23 (1976).
[8] P. R. Strutt and B. H. Kear, in *High-Temperature Ordered Intermetallic Alloys,* MRS Symp. Proc. Vol. 39, edited by C. C. Koch, C. T. Liu, and N. S. Stoloff (MRS, Pittsburgh, 1985), p. 279.
[9] *Superalloys II,* edited by C. T. Sims, N. S. Stoloff, and W. C. Hagel (Wiley, New York, 1987).
[10] G. Sauthoff, Z. Metallkd. **77**, 654 (1986).
[11] M. Takeyama and C. T. Liu, J. Mater. Res. **5**, 1189 (1990).
[12] S. R. Schuon and V. Rehzets, in *High-Temperature Intermetallic Ordered Alloys III* (Ref. 4), p. 647.
[13] R. Yang, J. A. Leake, and R. W. Cahn, J. Mater. Res. **6**, 343 (1991), and references therein.
[14] R. Marazza, R. Ferro, and G. Rambaldi, J. Less-Common Met. **39**, 341 (1975).
[15] K. Vedula, V. Pathare, I. Aslanidis, and R. H. Titran, in *High-Temperature Intermetallic Ordered Alloys III* (Ref. 4), p. 411.
[16] H. R. Pak, C. W. Chen, O. T. Inal, K. Okazaki, and T. Suzuki, Mater. Sci. Eng. **A104**, 53 (1988).
[17] N. C. Tso and J. M. Sanchez, in *High-Temperature Intermetallic Ordered Alloys III* (Ref. 4), p. 63.
[18] B. P. Burton, J. E. Osburn, and A. Pastural, in *High-Temperature Intermetallic Ordered Alloys IV,* MRS Symp. Proc. Vol. 213, edited by L. A. Johnson, D. P. Pope, and J. O. Stiegler (MRS, Pittsburgh, 1991), p. 107.
[19] W. Kohn and L. J. Sham, Phys. Rev. **140**, A1133 (1965).
[20] O. K. Andersen, Phys. Rev. B **12**, 3060 (1975).
[21] L. Hedin and B. I. Lundqvist, J. Phys. C **4**, 2064 (1971).
[22] O. Kubaschewski, E. L. Evans and C. B. Alcock, *Metallurgical Thermochemistry* (Pergamon Press, Oxford, England, 1967), 4th ed.
[23] J. H. Xu, T. Oguchi, and A. J. Freeman, Phys. Rev. B **36**, 4186 (1987).
[24] P. Villars and L. D. Calvert, *Pearson's Handbook of Crystallographic Data for Intermetallic Phases* (American Society for Metals, Metals Park, OH, 1986).
[25] L. Vegard, Z. Phys. **5**, 17 (1921).
[26] See, for example, J. A. Alonso and N. H. March, *Electrons in Metals and Alloys* (Academic, San Diego, 1989), p. 242; J. H. Xu and A. J. Freeman, Phys. Rev. B **40**, 11 927 (1989).
[27] T. Hong, T. J. Watson-Yang, X. Q. Guo, A. J. Freeman, and T. Oguchi, Phys. Rev. B **43**, 1940 (1991); T. Hong, T. J. Watson-Yang, A. J. Freeman, T. Oguchi, and J. H. Xu, *ibid.* **41**, 12 462 (1990).

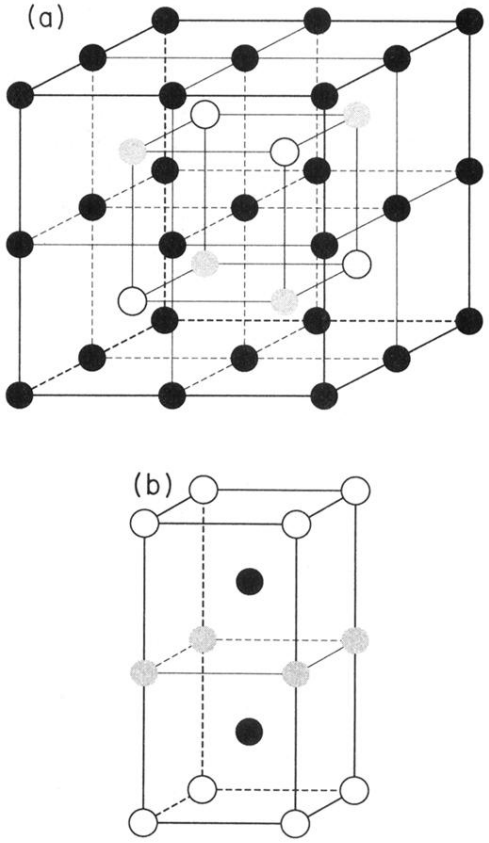

FIG. 1. The unit cell of the (a) $L2_1$ Heusler and (b) $B2$-like phase structure. The filled, shaded, and empty circles represent Ni, X, and Al atoms, respectively (X stands for Ti, V, Zr, Nb, Hf, and Ta).